$Eu:CaF_2$ layers on p-Si(100) grown using molecular beam epitaxy as materials for Si-based optoelectronics

T. Chatterjee,[a] P. J. McCann, and X. M. Fang
School of Electrical and Computer Engineering and Laboratory for Electronic Properties of Materials, University of Oklahoma, Norman, Oklahoma 73019

M. B. Johnson
Department of Physics and Astronomy and Laboratory for Electronic Properties of Materials, University of Oklahoma, Norman, Oklahoma 73019

(Received 22 December 1997; accepted 27 January 1998)

$Eu:CaF_2$ layers have been grown epitaxially on Si using molecular beam epitaxy (MBE) with the intent of realizing an electrically pumped optical source on Si. Here we present an atomic force microscopy study of the morphological features of MBE-grown $Eu:CaF_2$ on p-type Si(100) substrates and a study of electroluminescence (EL) from EL devices fabricated from these layers. The surface morphologies of the MBE-grown layers show an increased density of faceted features with increase in epilayer Eu content. X-ray photoelectron spectroscopy (XPS) data reveal the emergence of satellite peaks around the regular Eu XPS peaks in $Eu:CaF_2$ layer with high Eu content. The characteristics of EL devices fabricated on these layers is presented and a possible EL mechanism is discussed. © *1998 American Vacuum Society.* [S0734-211X(98)09403-7]

I. INTRODUCTION

Interest in molecular beam epitaxy (MBE) grown rare-earth doped CaF_2 is due in part to the possibility of incorporating large concentrations of rare earth ions in these layers without causing luminescence quenching. CaF_2 MBE growth temperatures are typically lower than the CaF_2 melting point by $\sim$1000 °C, and this inhibits rare earth ion clustering. MBE-grown CaF_2 layers containing Er^{3+} and Nd^{3+} have been studied in the past[1–4] with the aim of realizing solid state infrared light emitters on silicon having emission wavelengths suitable for coupling into optical fibers. The first report of MBE-grown $Eu:CaF_2$ layers on Si(111) was made by Sokolov *et al.*[5] wherein the position of the zero phonon line (ZPL) photoluminescence (PL) peak of Eu^{2+} was used to monitor strain in the CaF_2 layer. In later studies[6,7] it was shown that for MBE-grown $Eu:CaF_2$ layers, the integrated 10 K PL intensity of the Eu^{2+} vibronic side band increases with Eu content up to 7.5 at. % Eu. Recently, room temperature visible dc electroluminescence (EL) has been reported from these layers with Eu contents of 7.5 and 8.0 at. % Eu.[8] In this article we report studies of morphological features of MBE-grown $Eu:CaF_2/Si(100)$ layers using atomic force microscopy (AFM) and the EL emission spectra from EL devices fabricated with this material. Compatibility with standard silicon processing techniques makes this a promising materials system for integration of optical emitters with silicon circuitry.

II. EXPERIMENT

Growth of Eu-doped CaF_2 on Si(100) substrates was carried out in an Intevac Modular GEN II MBE system with a background pressure of $\sim 10^{-10}$ Torr during growth. Boron doped p-type 3-in-diam Si substrates with $<0.5°$ miscut and resistivities of (1–20 Ω cm) were cleaned using the Shiraki method, followed by a 10 s dip in a 10% HF solution. A well defined Si(100) (2×1) reflection high-energy electron diffraction (RHEED) pattern was observed after heating the substrate in UHV at 700 °C for $\sim$20 min. High-purity polycrystalline CaF_2 and elemental Eu were coevaporated from separate effusion cells to achieve compositional control and the Si substrate temperature was kept at 580 °C during growth. The structures of all the samples studied were comprised of a 400 Å undoped CaF_2 buffer layer, a 3600 Å $Eu:CaF_2$ layer, and a 200 Å undoped CaF_2 cap layer. These layers were annealed *in situ* at 1100 °C for 2 min to improve surface morphology as evidenced by the development of streaky RHEED patterns.[7]

XPS data were obtained from an adjoining analysis chamber using an Al $K\alpha_{1,2}$ x-ray source ($h\nu$=1486.6 eV) and a VG100AX hemispherical electron energy analyzer. AFM was done *ex situ* in air in contact mode using a Topometrix Explorer II microscope with a Si_3N_4 tip having a radius of curvature of 50 nm and a 45° slope. EL devices were fabricated by evaporating 500-μm-diam semitransparent aluminum dots on the as-grown MBE layer structures and the backs of the Si substrates were metallized with aluminum. These metallized layers were annealed in forming gas (20% hydrogen, 80% nitrogen) for $\sim$2 min at 450 °C. The EL spectra were recorded using an Ocean Optics S2000 spectrometer with a 360–850 nm grating and a 2048 pixel Si charged-coupled device (CCD) array with a 0.3 nm resolution. An optical fiber was used to collect the EL signal and couple the light to the spectrometer. The EL spectra were corrected for the spectral response of the collection optics and spectrometer.

[a]Electronic mail: t-chatterjee@ti.com

 0734-211X/98/16(3)/1463/4/$15.00 ©1998 American Vacuum Society

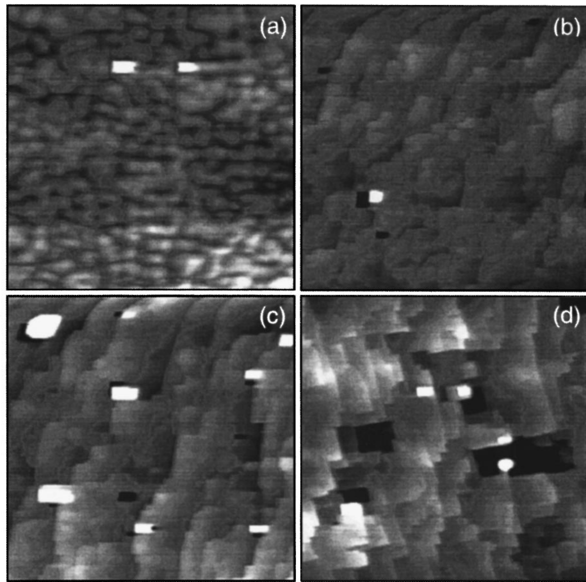

FIG. 1. AFM scans of MBE grown Eu:CaF_2/Si(100) layers containing 0, 1.0, 4.0, and 7.5 at % Eu are shown in (a)–(d), respectively. The scan areas are 10 μm$\times$10 μm and the gray scale used in the image represents vertical heights in the range of 0–30 nm.

III. RESULTS AND DISCUSSION

A. Surface morphology

Figures 1(a)–1(d) show the AFM scans from four MBE-grown Eu:CaF_2/Si(100) samples containing 0, 1.0, 4.5, and 7.5 at. % Eu. The Eu contents in these layers are estimated from beam flux and XPS measurements as described elsewhere.[7] The features seen in the 10 μm$\times$10 μm AFM scans are representative of larger area scans (100 μm $\times$100 μm). The surface morphology shows a definite trend with increase in Eu content. The samples with higher Eu content show a higher density of faceted features which have also been observed by scanning electron microscopy (SEM). Detailed line scans of these features from samples containing 4.0 and 7.5 at. % Eu are shown in Fig. 2.

Figure 2(a) shows the AFM image of a pyramidal facet and an adjoining depression from a 4.0 at. % Eu sample, and horizontal (X scan) and vertical (Y scan) line scans across the AFM image, both of which are along $\langle 110 \rangle$ directions. The features seen in Fig. 2(a) are common to all Eu:CaF_2 and undoped CaF_2 layers grown on Si(100), however, the density of these features increase with an increase in Eu content as seen in Fig. 1. The horizontal line scan (X scan) in Fig. 2(a) shows that the two opposite faces of the pyramidal structure along the direction of the scan are at a $\sim$26° angle with respect to the substrate, whereas the upper vertical scan (Y scan, scan 1) shows that one of the faces of the pyramid is inclined to the surface at an angle of 36°, while the other is inclined at an angle of 26° to the surface of the substrate. It should be noted that the depression adjacent to the pyramid-like structure has a maximum depth of $\sim$35 nm. A similar asymmetry is seen in the slopes of this depression in the lower vertical line scan (Y scan, scan 2) in Fig. 2(a) through that feature. Figure 2(b) shows a line scan through a typical faceted area from the 7.5 at. % Eu layer. This feature has more structure than the one in Fig. 2(a), but the shapes and angles are very similar. Step heights of $\sim$20 nm can be resolved in the smoother regions of the surface from this scan. Based on the angles measured by the AFM scans in Fig. 2(a) we conclude that this pyramidal structure does not arise from (111) planes intersecting a (100) surface.

It is interesting to note that the angle of inclination of a (111) plane with respect to a (110) plane is 35.26°. In fluorites, the $\langle 111 \rangle$ surfaces have the lowest surface energy and the exposure of these surfaces produces a thermodynamically favorable surface morphology. In a TEM study of MBE grown CaF_2 on Si(100)[9] it was shown that quasi-one-dimensional CaF_2 islands nucleate on Si(100) surfaces. These islands have a (110) plane as their base and their exposed faces are comprised of intersecting (111) planes. Although such a structure can explain the inclination of one of the faces (36°) seen in the pyramidal structure in Fig. 2(a), it does not explain the inclination of the other faces (all of which are $\sim$26°). It therefore seems that the pyramidal structures in Eu:CaF_2/Si(100) may have a different origin.

The smoothing of MBE grown CaF_2/Si(100) layers using rapid-thermal annealing has been conjectured to be due to the formation of a large number of Schottky defects which distribute in the CaF_2 layer in such a way as to reduce the dipole moment of the (100)-oriented surfaces and making them thermodynamically stable.[10] The interaction of these defects with Eu in the CaF_2 layers can produce complex defect equilibria which in turn can affect the density of morphological features on the Eu:CaF_2 epilayers. This may explain the observed dependence of roughness on Eu content.

The AFM study presented here shows that the morphological features on the surface of Eu:CaF_2 layers do not have aspect ratios that can significantly enhance field emission when metal electrodes are deposited. It is also seen that the epilayer thickness under the depressions which are adjacent to the pyramidal facets can be $\sim$10% less than the epilayer thickness in the smoother regions of the surface. Therefore, local electric fields in the epilayer below these depressions will be higher than the electric field in the rest of the epilayer. Since Eu:CaF_2 layers with high Eu content have a high density of these depressions, it is conceivable that any current injection mechanism produced by such a local enhancement of electric field will be more pronounced in these layers, and could provide high-energy carriers for impact excitation of optical centers in the epilayer underneath these depressions. A study of EL intensity versus epilayer thickness is needed to test this hypothesis.

B. XPS Eu peaks

The Eu $3d_{3/2}$ and $3d_{5/2}$ peaks from the XPS spectra of Eu:CaF_2/Si(100)-p samples containing 1.0, 4.0, 8.0, and 12.0 at. % Eu are shown in Fig. 3. It can be seen that two satellite peaks emerge on both the high and low binding energy side of the Eu $3d_{5/2}$ peaks for the spectra from 7.5 and 12.0 at. % Eu samples. The higher and lower binding

FIG. 2. (a) Phase contrasted AFM image and line scans through a pyramidal facet on a 4.0 at % Eu:CaF_2/Si(100) layer are shown in (a). The line scans (X scan and the Y scans) were along ⟨110⟩ directions. The scan area was 1 μm×1 μm. (b) A phase contrasted AFM image and a line scan through a faceted feature on a 7.5 at % Eu:CaF_2/Si(100) layer are shown in this figure. The scan area was 3 μm×3 μm.

energy XPS satellite peaks may be associated with a Eu defect complex or different charge states of the Eu atom, although the higher binding energy satellite peak could also arise from an inelastic electron scattering process. The possibility of Eu being in different charge states in Eu:CaF_2 layers with high Eu content and the fact that strong EL is seen from Eu:CaF_2 layers with high Eu content suggests that the EL mechanism may involve the excitation of an Eu center that is not present in the lightly doped Eu:CaF_2 layers.

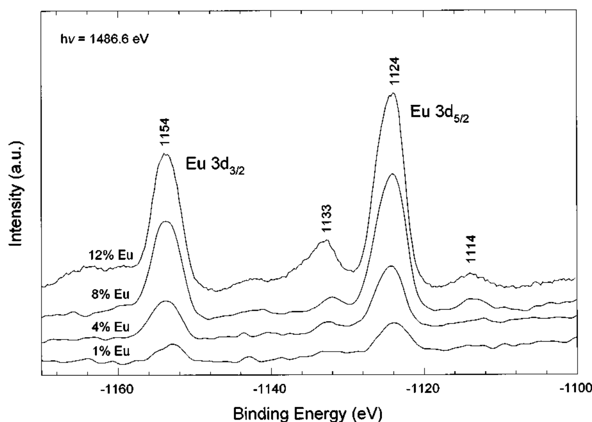

FIG. 3. Eu $3d_{3/2}$ and $3d_{5/2}$ XPS peaks are shown as a function of Eu content in at %. The position of all prominent peaks are indicated in the figure in terms of their absolute binding energy in eV.

C. Electroluminescence (EL)

Room temperature EL spectra under different dc biases for an EL device made from Eu:CaF_2/Si(100)-p containing 8.0 at. % Eu and provided with semitransparent aluminum electrodes, are shown in Fig. 4. The inset in Fig. 4 shows the integrated EL intensity as a function of applied bias. A threshold of ~15 V can be seen in this curve after which the EL intensity increases linearly with applied voltage. EL from this device was obtained with the aluminum electrode held at a negative bias relative to the Si substrate. Reversing the polarity of the bias and applying similar voltages produced very faint EL with no measurable change in the shape of the EL spectrum. The magnitude of the injection current was independent of the polarity of the bias and the current varied almost linearly with applied bias in the region where EL was

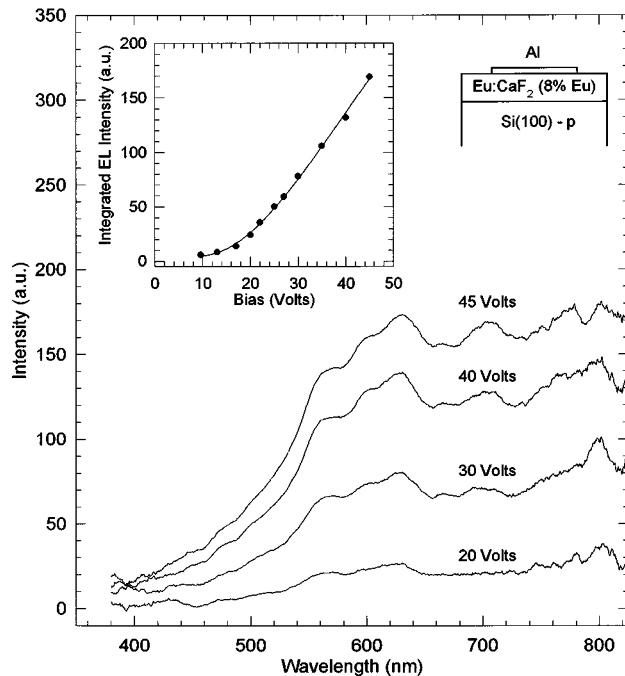

FIG. 4. Room temperature EL spectra as a function of applied bias is shown in this figure for an EL device fabricated from 8.0 at % Eu:CaF_2/Si(100) structure with a semitransparent aluminum electrode. The inset shows a plot of integrated EL intensity vs applied bias for this device. The EL device structure is also shown in the figure. The aluminum electrode was biased negative relative to the Si(100)-*p* substrate for all the data shown in this figure.

observed. Similar EL devices have also been fabricated using Eu:CaF_2 layers containing 7.5 and 4.0 at. % Eu. The EL intensity from the device with 4.0 at. % Eu is much weaker than the EL from devices made with Eu:CaF_2 layers containing 7.5 and 8.0 at. % Eu.

The room temperature PL spectra of Eu:CaF_2 layers, containing 1.0 to 8.0 at. % Eu, obtained with uv excitation (~365 nm) reveal strong emission from Eu^{2+} ions in the CaF_2 lattice which peaks at 425 nm,[11] indicating that a significant concentration of the Eu atoms in these layers are in their +2 charge state. The EL spectra on the other hand are very broad and show structure around 560, 600, 620, 700, and 800 nm. Optical emission from Eu^{3+} sites in CaF_2 have peaks around 520, 600, 620, 650, 700, 750, and 800–850 nm.[12] In a study of Ar ion induced luminescence from bulk CaF_2 crystals, ion implanted with Eu,[13] it was demonstrated that impact excitation of Eu^{3+} in CaF_2 produces optical emission, with two broad peaks centered around 600 and 700 nm. Thus, electron impact excitation of Eu^{3+} ions in the MBE-grown Eu:CaF_2 layers can explain the features of the EL spectra shown in Fig. 4. This would be consistent with the presence of higher binding energy satellite peaks in the Eu XPS spectra, which may indicate the existence of Eu centers which are in a +3 state.

IV. CONCLUSIONS

MBE-grown Eu:CaF_2/Si(100) layers have been used to fabricate EL devices on Si. The surfaces of Eu:CaF_2 layers, as seen from the AFM study, show an increase in the density of faceted structures with increase in Eu content. Although strong EL is obtained from samples with high Eu content, it is not clear whether the faceted features present on the surface of Eu:CaF_2 layers with high Eu content play a role in the EL mechanism. The presence of features in the EL spectra which coincide with the emission peaks of Eu^{3+} and the possibility of Eu being in different charge states for samples with high Eu content suggest that luminescence from Eu^{3+} could be responsible for EL from Eu:CaF_2/Si(100) samples with high Eu content. The demonstration of visible EL using dc excitation makes Eu:CaF_2/Si(100) a promising materials system for Si-based display applications. Future work towards definite identification of an EL mechanism and the nature of current conduction through the structure will help optimize EL device performance.

ACKNOWLEDGMENTS

The authors thank Shane Lundstrom for help with the AFM scans and Amy Liu for providing some of the XPS data. This work was supported by NSF EPSCoR under Grant Nos. OSR-9108771 and OSR-9550478.

[1]L. E. Bausa, R. Legros, and A. Munoz-Yague, Appl. Phys. Lett. **59**, 152 (1991).
[2]L. E. Bausa, C. Fontaine, E. Daran, and A. Munoz-Yague, J. Appl. Phys. **72**, 499 (1992).
[3]C. C. Cho, W. M. Duncan, T. H. Lin, and S. K. Fan, Appl. Phys. Lett. **61**, 1757 (1992).
[4]E. Daran, R. Legros, A. Munoz-Yague, C. Fontaine, and L. E. Bausa, J. Appl. Phys. **76**, 270 (1994).
[5]N. S. Sokolov, N. L. Yakovlev, and J. Almeida, Solid State Commun. **76**, 883 (1990).
[6]X. M. Fang, T. Chatterjee, P. J. McCann, W. K. Liu, M. B. Santos, W. Shan, and J. J. Song, J. Vac. Sci. Technol. B **14**, 2267 (1996).
[7]X. M. Fang, T. Chatterjee, P. J. McCann, W. K. Liu, M. B. Santos, W. Shan, and J. J. Song, Appl. Phys. Lett. **67**, 1891 (1995).
[8]T. Chatterjee, P. J. McCann, X. M. Fang, J. R. Remington, M. B. Johnson, and C. Michellon, Appl. Phys. Lett. **71**, 3610 (1997).
[9]D. Loretto, F. M. Ross, and C. A. Lucas, Appl. Phys. Lett. **68**, 2363 (1996).
[10]X. M. Fang, P. J. McCann, and W. K. Liu, Thin Solid Films **272**, 87 (1996).
[11]T. Kobayasi, S. Mroczkowski, and J. F. Owen, J. Lumin. **21**, 247 (1980).
[12]R. J. Hamers, J. R. Wietfeldt, and J. C. Wright, J. Chem. Phys. **77**, 683 (1982).
[13]K. Aono, M. Iwaki, and S. Namba, Nucl. Phys. B **32**, 231 (1988).